Journal of Metals, Materials and Minerals, 36(3), e2537, 2026

Effect of MgO on crawling and physical properties in ceramic glazes

Thongpanchang TIMCLUB[1], Pathitta ANURAKSOMBAT[1], Thatree MUANGKAEW[2], Niti YONGVANICH[1,*]

[1] *Department of Materials Science and Engineering, Faculty of Engineering and Industrial Technology, Silpakorn University, Nakornpathom, 73000 Thailand*

[2] *Department of Ceramics, Faculty of Decorative Arts, Silpakorn University, Nakornpathom, 73000 Thailand*

***Corresponding author e-mail**: niti@su.ac.th; niti.yongvanich@gmail.com

Received date:
22 December 2025
Revised date:
2 February 2026
Accepted date:
27 February 2026

Keywords:
Crawling;
Defect;
Phase formation;
Ceramic glaze

Abstract

This study attempted to seek and verify the scientific aspects responsible for crawling in ceramic glazes. The selected additive was magnesium oxide (MgO). The glazes were applied on porcelain biscuits and fired between 1100°C and 1300°C. The degree of crawling was enhanced with increasing amount of MgO, which was accompanied by formation of forsterite (Mg_2SiO_4) as a major phase. Complete island separation was achieved with 10 wt% MgO with good wettability and shiny surface. The morphology of the glaze demonstrated this phase as small crystals within the glaze layer. Addition of MgO resulted in a continuous decrease in the thermal expansion coefficient (as low as 11.76×10^{-6} 1·°C^{-1}) likely due to crystallization of different phases. On the contrary, both glass-transition and softening temperatures (T_g and T_s) showed an initial decrease when adding 5 wt% MgO. However, the trend was reversed beyond the amount of 10 wt%. The in-depth study of the glass structure could not be carried out as the crystalline phase generating Raman peaks that interfered the deconvolution of the non-bridging oxygen (NBO) characteristics. The melting behavior displayed a similar trend to both T_g and T_s, signifying the complicated role of Mg cations in the glaze structure. Addition of MgO (5 wt%) could reduce the softening temperature from 1082°C to 987°C suggested that a small amount of MgO could likely behave as a network modifier. A higher amount modified the glaze structure to be closer to a glass-creamic. This change in phasic nature was likely to yield the glazes with high rigidity, high surface tension via melting difficulty which were closely reflected by the increase in the thermal expansion coefficient as well as T_g and T_s. Formation of crystalline phases due to MgO addition was believed to mainly cause crawling as evidenced by various, relevant characterization techniques.

1. Introduction

Glazing is one key step in the processing of ceramic products with purposes aiming for both functionality and decoration. A typical glaze layer forms upon reaching the maturation temperature as a glass-like or amorphous silicate film covering a clay body. Such formation can yield enhancement in strength, suitability for food storage and embellishment for value addition. Ceramic glazes can be categorized differently depending on the context of consideration. Visual appearance tends to be more useful in glaze classification as it encompasses attributes relevant to physical characteristics such as surface texture (matt or shiny), coloration, crystallization or topographical feature.

One of the unusual glaze effect that has been considered as a defect is a crawl glaze. This type of glaze has a characteristic of island-like landscape within which the glaze layer was separated from each other into patches, exposing the underlying clay. Depending on the level of glaze maturation and composition, the glaze's topography might resemble a parched land with cracking whose surface could be either sharp or curved. Other names used by artists are lichen and lizard's skin. It should be noted that glaze crawling can be either intentionally induced for a desired effect or unintendedly obtained from imperfection of glaze application prior to firing. This first can be achieved by deliberate adjustment of the formulation whereas the latter is usually associated with the aspects beyond the glaze chemistry such as uncleaned clay surface or unusually thick glaze layering. This study would only focused on the first case where crawling was primarily caused by tailoring the glaze recipe via compositional adjustment.

The phenomenon of crawling in ceramic glazes has been reported to be caused by several reasons. However, the number of published articles is very limited, and there is still a lack of in-depth investigation into the correlation between the raw materials, structure and processing. Youssef *et al.* [1] characterized crawling as the discontinuity of the glaze layer, leaving a bare area in the glazed body. They explained that crawling could be caused by several reasons such as an interruption in the continuity of the glaze thickness, the glaze particle size and the surface tension. Other possible reasons included high viscosity of the melted glaze, the presence of too much alumina or soluble salts in the glaze or even a long cycle with a slow cooling. The effect of particle size on crawling was examined by Wattanasiriwech and Wattanasiriwech [2]. In their glaze containing no MgO, prolonged milling of glaze powder (up to 16 h) resulted in a glaze crawling. Although no mechanism on crawling was stated, they believed that

such crawling was caused by the increase in viscosity and surface tension. Crawling in the Shino glaze was reported by Junta *et al.* [3] by addition of Al_2O_3, $CaCO_3$ and $MgCO_3$. Only $MgCO_3$ was found to induce crawling and the authors attributed this effect to the high surface tension forces. The formation of a new phase ($MgSiO_3$) was proposed but without the X-ray Diffraction patterns. Surface tension was also emphasized to be a key property for glaze processing by Li *et al.* [4]. The increase in surface tension from extreme particle size reduction resulted in air capsulation induced by a strong interaction of molten glaze and the air. These air bubbles were stated to be able to cause crawling.

Among these published reports, the attributes to crawling were focused on particle size reduction, the type of additive ($MgCO_3$), surface tension and glaze-air interaction. Given the glaze firing is a complex process, to shed light on the real mechanism of crawling, one needs to design the experiment carefully. Investigation on intrinsic factors pertinent during glaze melting such as surface tension, phase formation and morphology should be prioritized over other extrinsic factors (cleanliness of the body, starting particle fineness and firing cycle). In addition, the issue of thermal expansion should also be examined as this property has been known as a culprit in glaze crazing and peeling. This issue of thermal mismatch has been in discussion among potters and artists as well. The understanding of this thermal property would be valuable in term of glass science as it would allow a much deeper insight toward alteration in the glass structure itself especially the coefficient of thermal expansion, the glass-transition temperature and the softening temperatures. Therefore, this study aimed to systematically examine the effect of MgO addition on glaze crawling. Based on the materials science paradigm, this study attempted to establish a correlation among phase formation, morphological structure, thermal property and glass structure in order to possibly shed a light on the science behind glaze crawling at some levels.

2. Experimental

The chemicals used in this study were industrial-grade with 325 mesh granulation: Nepheline syenite ($(Na,K)AlSiO_4$, Amarin), Kaolin ($Al_2Si_2O_5(OH)_4{\cdot}2H_2O$, Amarin) and Magnesium oxide (Amarin). The general formula was (0.95-x)[Nepheline syenite + (0.05)[Kaolin] + (x)[MgO] where x is a weight fraction with values being 0, 0.05, 0.1, 0.2 and 0.3. Boron oxide was added in the amount of 2 wt% for all compositions to aid glaze maturation in the range of cone 5 and 6. The stoichiometric mixtures were ball-milled using alumina balls and distilled water in HDPE bottles for two hours after which they were oven-dried at 120°C for 24 h. The particle size distribution was probed by a Dynamic Light Scattering Particle Size Analyze (Coulter, LS-100Q) with water as a medium. All firings were carried out in an electric furnace with ramping rates of 200 $°C{\cdot}h^{-1}$. Clay biscuits were approximately 5 cm. in diameter and were slip-casted from porcelain (Compound Clay, PFA casting type). This size allows sufficient observation of any surface defects that might occur. After drying for two days, the biscuits were bisque-fired at 800°C for 1 h. The prepared glaze slips were made of the previously prepared glaze powders and had a specific gravity of 1.4 with their volumes measured to be five milliliters for each biscuit. The samples were fired at 1200°C for 1 h to yield samples with a different degree of crawling and maturation.

To investigate the phase formation, the glaze powders were put in a porcelain crucible and fired at 1200°C for 1 h. After firing, the samples were carefully removed by crushing, obtaining only the parts that did not contain the crucible's material. The small lumps were hand-ground in an agate mortar with acetone as a medium. The obtained fine powders were applied on a frosted glass slide for X-ray Diffraction (XRD, Shimadzu 6100). The XRD scanning conditions were 10 degree to70 degree (step scan of 0.02 degree) with the current of 30 A and the voltage of 40 V. The surfaces of the fired glaze samples were also examined by XRD. Due to the crawling feature, the rough and wavy surfaces were deemed to be unsuitable for XRD technique. Hence, this study used the results from the crushed sample as a representative of the glaze samples themselves. For the morphological study, the glaze samples were etched using HF to remove the glassy layer covering the top part of the glaze as well as the glass portion underneath in order to clearly observe any crystalline particles within the glaze.

The microstructure was examined by a Scanning Electron Microscope (SEM, TESCAN - MIRA3) with elemental analysis. The thermal property was characterized by Dilatometry (NETZSCH DIL 402) which yielded the glass-transition temperature (T_g), the softening temperature (T_s) and the coefficient of thermal expansion (CTE). Dilatometric samples were prepared from the previously obtained powders used for XRD. These powders could be considered to be similar to frits. They were consolidated into a small rod-shape graphite mold and fired at 1000°C for 1 h. This method of sample preparation did not result in any significant alteration in phasic nature compared to those from the previous XRD characterization.

Raman Spectroscopy was employed to investigate the glass structure itself. Unfortunately, because addition of MgO induced formation of several crystalline phases, analysis on the non-bridging oxygen (NBO) of the amorphous portion was only possible for the x = 0 and 0.05 samples. To understand the effect of MgO addition on the melting behavior, the unfired glaze powders were pelletized into a cylindrical shape of 15 mm. in diameter with a height of approximately 10 mm. These pellets were fired at different temperatures between 1000°C and 1300°C for 1 h. Reduction in height was utilized as a measure of the degree of sintering and melting, yielding different characteristic temperatures crucial for glaze maturation that was analogous to the hot-stage microscopy technique.

3. Results and discussion

As previously reported, glaze crawling could be induced by the fineness or particle size of the glaze powders [2]. Hence, the information on the particle size used in each study of glaze crawling should be fully characterized. The employed glaze mixtures in this current study were passed through a 325 mesh sieve with no residues; all starting raw materials were also of 325-mesh specification. Figure 1 displays the SEM images of the x = 0.1 powdered sample at different magnifications. The particle morphology varied according to the three different stating raw materials (Nepheline syenite, kaolin and MgO). The particle size ranged from less than a micron to as large as 20 μm. This range was in agreement with the particle size distribution result shown in Figure 2.

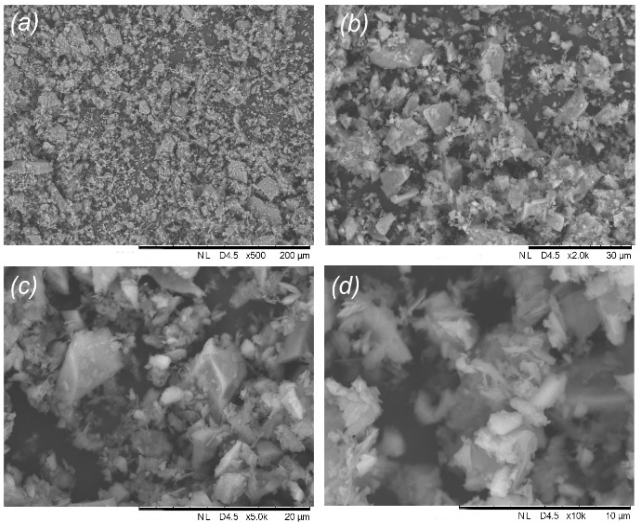

Figure 1. SEM images of the x = 0.1 glaze powders used in this study at different magnifications. Other compositions revealed relatively similar sizes. (a) 500x, (b) 2000x, (c) 5000x, and (d) 10000x.

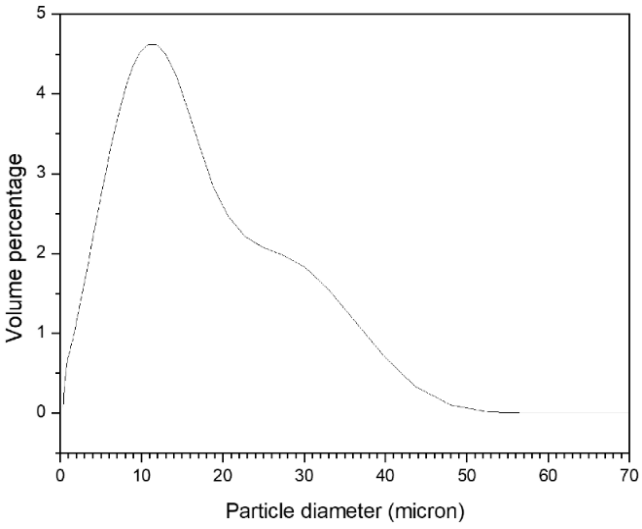

Figure 2. The particle size distribution of the x = 0.1 glaze powders using the Fraunhofer mode.

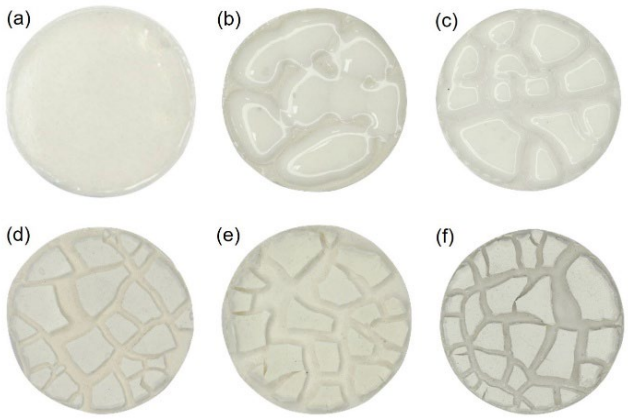

Figure 3. Glaze samples with different amounts of MgO addition fired at 1200°C for 1 h. (a) 0 wt%, (b) 5 wt%, (c) 10 wt%, (d) 15 wt%, (e) 20 wt%, and (f) 30 wt%.

The data revealed that all detected particles (or agglomerates induced by water) were primarily smaller than 50 μm with the mean, median and mode values being 11.43 μm, 9.20 μm and 11.29 μm, respectively. These values were within the same range as that obtained by SEM. The obtained graph demonstrated the skewness being 1.3 right skewed and the kurtosis being 1.58 Leptpkurtic. The majortity of the particles (90%) was smaller than 24.73 μm, which further confirmed the fineness of the 325 mesh quality of the starting glaze powders.

MgO addition has a profound effect on the physical morphology of the glazes. Without MgO, no crawling was observed; the glaze appeared to be similar to a typical clear glaze. The glaze started to crawl when adding MgO as shown in Figure 3. The x = 0.05 sample (5 wt% MgO) yielded different glaze islands among which are still inter-connecting with each other. Total separation of all islands occurred when increasing MgO addition to 10 wt% or more. The size of the islands remained virtually unchanged regardless of the amount of MgO; however, the glossiness gradually disappeared beyond the MgO addition of 10 wt%. In fact, the x = 0.2 and 0.3 samples contained glaze plates which were loosely adhered to the underlying clay substrate. They also appeared like a parched land with rough surface, signifying possible incomplete melting of the starting precursors. Although MgO has been assigned to be a network modifier (flux) according to the glass chemistry, its melt-facilitating role does not commence until the temperature reaches higher than 1200°C. Given this "auxiliary fluxing" nature, the current firing temperature in this study was still below the threshold required for MgO to take into action for the process of maturation. In addition, MgO's refractoriness (high melting point) is also another reason for affecting the eutectics, causing incomplete melting of the glaze mixture as evidenced by the "dry" and matt surface of the obtained glaze.

The glaze texture was further examined using the information on wetting angle, and coverage area. These characteristics could be deduced from the difference in island formation with different MgO addition. Only the low amounts of MgO (5 wt% and 10 wt%) would be examined as higher amounts resulted in warping of each island or plate. This occurrence left the perimeters untouching the underlying clay substrate, signifying inaccuracy in any attempt to characterize the glaze texture. The wetting angles were 39.2° and 34.3° for the x = 0.05 and 0.1 samples, respectively. The ability of the glaze to spread across a substrate suggested a higher degree of melting as demonstrated by the obvious amorphous halo in Figure 3. This "spreading" character was also reflected in an increase in the coverage area (using ImageJ software) from 86.04% to 92.10% for the x = 0.05 and 0.1 samples, respectively. Upon increasing the amount of MgO beyond 15 wt%, the size of the islands and the channel width remained relatively unchanged due to the refractoriness of the glaze.

The unique surface of the glaze was accompanied by compositionally dependent phase formation. Adding MgO to the base glaze induced several secondary phases to occur as demonstrated in Figure 4. The base glaze revealed only two phases which were mullite ($Al_6Si_2O_{13}$, JCPDS 15-0776) and albite ($NaAlSiO_8$, JCPDS 19-1184). These two phases were composed of all major elements present in the starting precursors and were likely to crystallize during cooling. With MgO in the amount of 5 wt%, the forsterite phase (Mg_2SiO_4, JCPDS 34-0189) started to emerged as tiny peaks. Other magnesium-containing phases started to form with higher MgO addition; they included enstatite

($MgSiO_3$, JCPDS 19-0768) and spinel ($MgAl_2O_4$, JCPDS 21-1152). The enstatite phase was also reported by Junta *et al*. [3] in their study on crawling of Shino glaze within which as much as 20% of MgO was added. The cristobalite phase (SiO_2, JCPDS 82-1410) was also detected which could be from incomplete maturation of the glaze. Beyond 10 wt% of MgO addition, the forsterite phase became a primary crystalline phase; its peak was becoming sharper with increasing MgO. The emergence of the forsterite phase starting with 10 wt% MgO was in agreement with the report by Wang *et al.* [5]; their study with small MgO addition (0.15 wt% to 5 wt%) only stated anorthite and diopside as main crystalline phases. The crystallite size from the peak's FWHM; however, could not be calculated because it was beyond the Scherrer's formula limit from the Warren broadening correction. Nevertheless, the XRD results suggested a possible correlation between the crystallinity and the level of crawling in this glaze system.

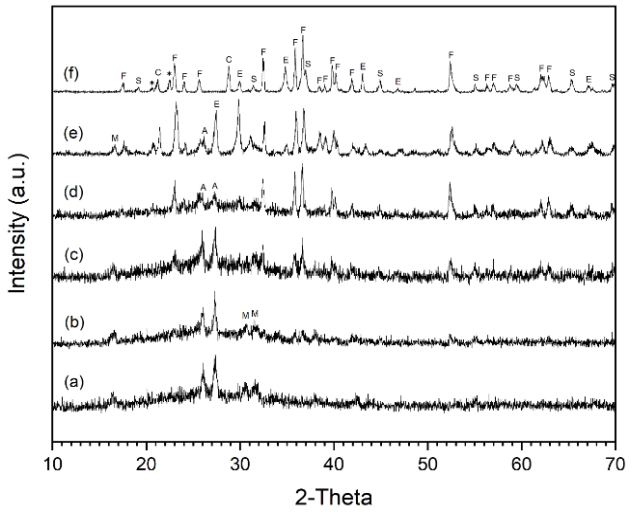

Figure 4. XRD patterns of glaze samples with different amounts of MgO addition fired at 1200°C for 1 h. (a) 0 wt%, (b) 5 wt%, (c) 10 wt%, (d) 15 wt%, (e) 20 wt%, and (f) 30 wt%. M = Mullite ($Al_6Si_2O_{13}$), A = Albite ($NaAlSi_3O_8$), C = Cristobalite (SiO_2), E = Enstatite ($MgSiO_3$), F = Forsterite (Mg_2SiO_4).

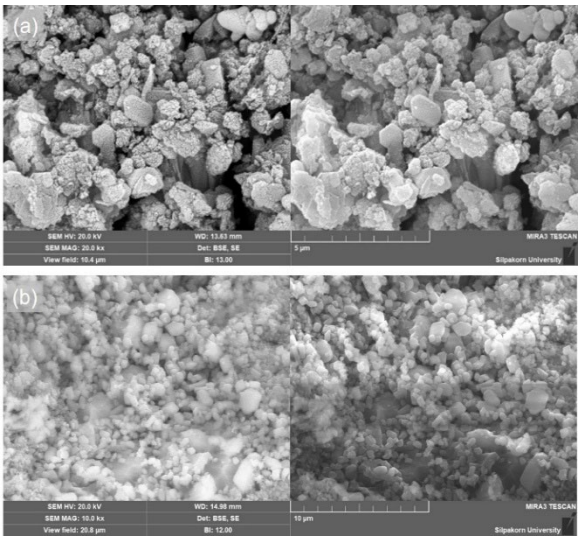

Figure 5. SEM images of the samples with different amounts of MgO addition fired at 1200 °C for 1 h. (a) 10 wt% with magnification of 20000x, and (b) 20 wt% with magnification of 10000x.

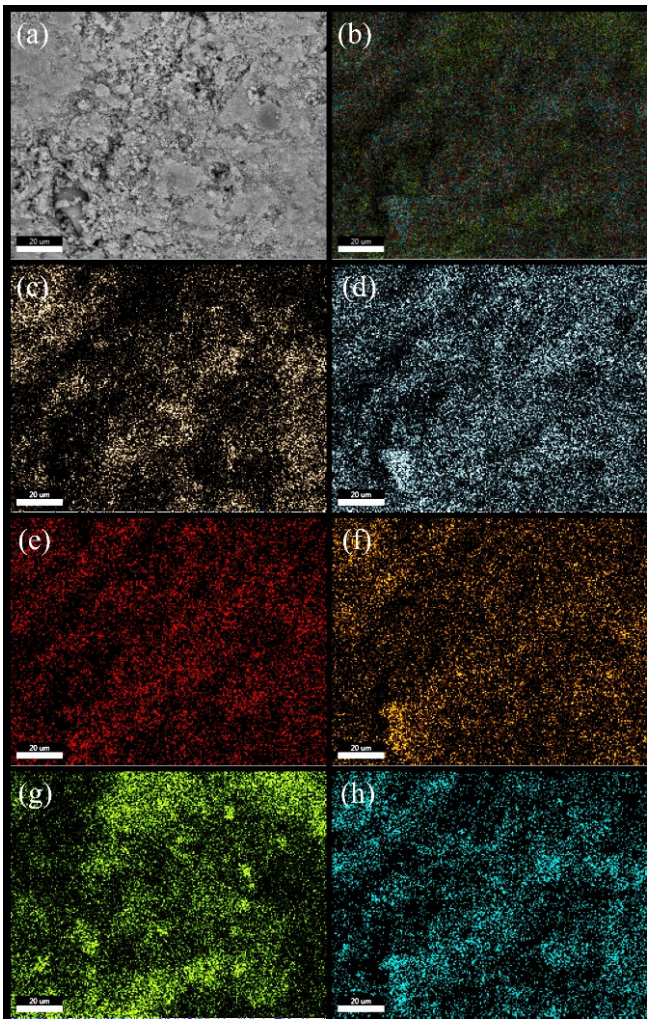

Figure 6. EDS mapping of the sample (x = 10 wt%) fired at 1200°C for 1 h. (a) The overall morphology, (b) Overlapping, (c) Mg, (d) Si, (e) Na, (f) Al, (g) K, and (h) O. The scale bar = 20 μm.

Forsterite as a major phase detected by XRD was clearly observed by Scanning Electron Micrsocopy (SEM) with elemental analysis. The morphology of the glazes (x = 0.1 and 0.2) was displayed in Figure 5. Both samples contained particles with different shapes and sizes which were in agreement with the XRD results (several phases detected). The porosity on the surface was caused by the etching process during which the glassy phase was removed. The particles were in a very wide size range between 200 nm to 20 µm, likely due to the variation in phase formation as detected by XRD. The EDS mapping of the overall sample revealed all elements present in the starting precursors. At a high magnification, particles with clear facets were observed and were confirmed by EDS (spotting mode) to be composed of Mg, Si and O. This EDS results suggested that these particles were forsterite as previously reported to be a major phase detected by XRD at high MgO amounts.

The microstructure revealed a relatively uniform distribution of all elements in the glaze. Figure 6 shows the EDS mapping of different elements for the x = 0.1 sample. The dark area was caused by acid etching from the SEM preparation. There was an area of intense signals of Al and Si (lower right in Figure 4(f-g) which was likely to be either albite or mullite according to the previous XRD results. Potassium (K) was also detected all over the sample which came from the composition

of the employed nepheline syenite itself that contained both Na and K. The phase of interest is forsterite (Mg_2SiO_4); its elements (Mg and Si) were found to be present in the EDS maps. It should be noted that the intensity of the Mg signals was stronger in some areas such as one the upper left and the middle right. This intense signals in these areas were also accompanied by the much denser structure as demonstrated in Figure 6(a). The EDS spectrum of the overall sample was shown in Figure 7. Contrary to the microstructural aspect of dense glassy phase, these areas were actually the agglomeration of Mg_2SiO_4 particles and would not have been a glass phase as the sample was already etched by HF. The presence of Mg_2SiO_4 was confirmed by EDS in the spotting mode (Figure 8) in those dense area to possess the composition relatively close to that of the stoichiometric forsterite (Mg 30.4%, Si 15.3% and O 54.3%) and was previously indexed by XRD.

MgO addition has a great effect on the thermal property of the glaze. The dilatometric profiles of all samples are shown in Figure 9 with a zoom-in in the 200°C to 500°C to demonstrate the difference in the slope of each sample as this range holds linearity. The samples beyond x = 0.2 were not carried out as they appeared to be so immature or incompletely melted that no accuracy could be obtained from dilatometry. The thermal expansion coefficient (α) of the base glaze (without MgO) was calculated in this temperature to be 16.7E-6 $1{\cdot}°C^{-1}$. The alpha value gradually decreased with increasing MgO amount to as low as 11.8E-6 $1{\cdot}°C^{-1}$ for the x = 0.2 sample. This monotonic reduction in alpha could likely be associated with the emergence of crystalline phases (albite, mullite and forsterite) as detected by XRD. The crystallization of these phases would have made the samples to be indistinguishable from glass-ceramics. Induced crystallinity during cooling in glass-ceramics was well-known to be responsible for an increase in the thermal expansion coefficient. In their characterization of glass-ceramic glazes, Rasteiro *et al.* [6] reported that the thermal expansion coefficient could be influenced by the presence and extent of crystallization. The ordering in the crystal structure (newly formed phases) tended to be more resistant to thermal vibration compared to that with amorphousness or glassy nature.

On the contrary, the glass transition temperature (T_g) and the softening temperature (T_s) revealed a different trend. They decreased first with MgO addition of 5 wt% and slowly increased with increasing MgO. Two additional samples with MgO addition of 2 wt% and 7 wt% were carried out in order to verify this non-monotonic trend. The lowest values of T_g and T_s occurred at x = 0.05 and were 710.1°C and 805.1°C, respectively. This reduction was possibly caused by the fact that magnesium cations could behave as a flux or network modifier according to the theory of glass chemistry. Although Mg is an auxiliary flux requiring the temperature higher than 1200°C to take effect, it was possible that the starting mixture contained some eutectics among different compounds. The absence of the starting MgO and reacting Mg_2SiO_4 phases in the XRD results suggested that the Mg cations were likely to be incorporated into the glass network, behaving as a modifier similar to alkali and alkali earth cations. The resulting weakening of the Si–O–Si network allowed the structural chain to be more sensitive to thermal perturbation at the glass transition temperature, yielding a decrease in T_g (transitions from a rigid, brittle state to a more viscous, rubbery state) The same mechanism could explain the similar trend in the T_s values as glass softening is defined to be the point where a certain viscosity allows the glass to be deformed under its own weight. Upon increasing the MgO amount beyond 5 wt%, both T_s and T_g gradually increased. This phenomenon was likely associated with the emergence of several crystalline phases formed as detected by XRD. These phases such as forsterite would have made that glass sample to become a glass-ceramic material similar to a composite. The presence of the crystalline entity within the amorphous matrix would hinder the ability of the glassy phase to deform at the softening point, resulting in a monotonic increase in both T_g and T_s.

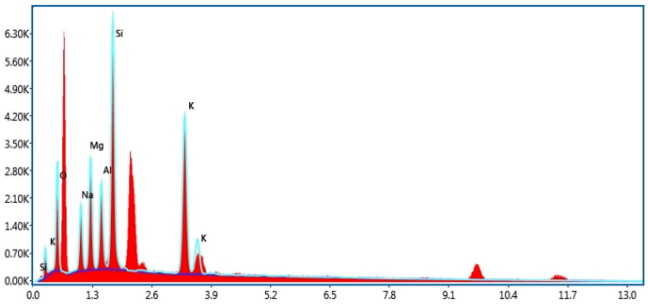

Figure 7. EDS mapping of the sample (x = 10 wt%) fired at 1200°C for 1 h.

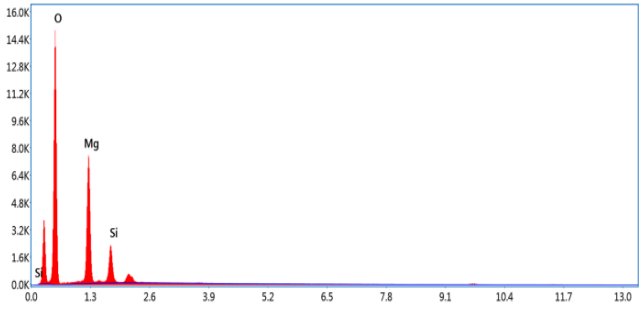

Figure 8. EDS in the spotting mode of the sample (x = 10 wt%) fired at 1200°C for 1 h. The probed area was in the particles observed in the SEM.

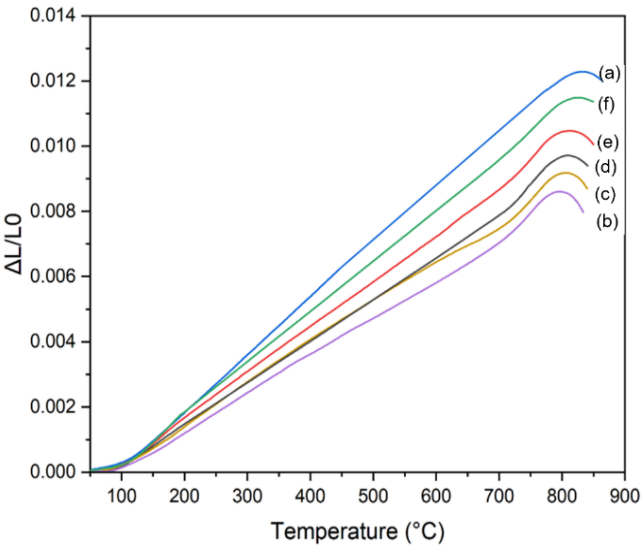

Figure 9. Dilatometric profiles of glaze samples with different amounts of MgO addition. (a) 0 wt%, (b) 2 wt%, (c) 5 wt%, (d) 7 wt%, (e) 10 wt%, and (f) 20 wt%. The x = 0.3 sample was too immature to be examined by dilatometry.

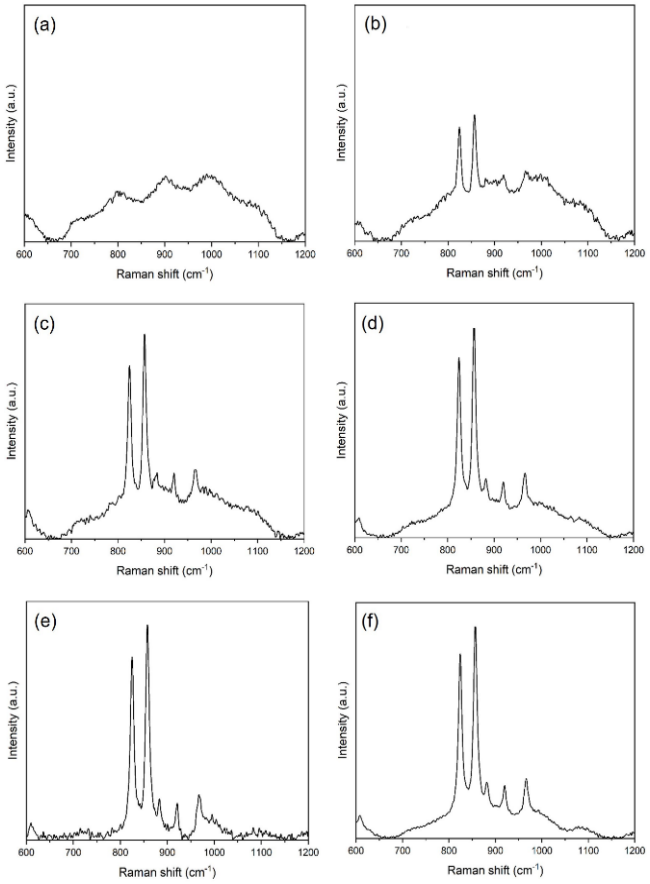

Figure 10. Raman spectra of glaze samples with different amounts of MgO addition fired at 1200°C for 1 h. (a) 0 wt%, (b) 5 wt%, (c) 10 wt%, (d) 15 wt%, (e) 20 wt%, and (f) 30 wt%.

Attempts have been made to examine the changes in the glass structure with MgO addition by using Raman spectroscopy (Figure 10). The glaze layers were carefully removed from the underlying clay substrate and were prepared in the same way as the XRD samples. The x = 0 sample yielded a profile similar to a regular silicate glass with one group of large peaks in the 600 cm^{-1} to 1200 cm^{-1} range. This profile could be deconvoluted into five individual peaks corresponding to Q^n where n is the number of non-bridging oxygen. Upon adding MgO, however, sharp peaks emerged at 824 cm^{-1}, 857 cm^{-1} and small peaks at 882 cm^{-1}, 920 cm^{-1}, and 966 cm^{-1}. These peaks were reported by Mouri and Enami [7] to be symmetric and asymmetric stretching of Si–O and Si–O–Mg in the forsterite (Mg_2SiO_4) structure. The positions of these forsterite peaks were overlapped with the Q^0, Q^1, Q^2 and Q^3 peaks associated with the silicate glass network. Therefore, no conclusive information regarding the influence of Mg cations on the glass structure could be drawn from these Raman results.

The effect of MgO addition on the melting behavior of the glazes was investigated by measuring the remaining height of the sample at different firing temperatures. Four characteristic temperatures relating to melting are the sintering point (95% height), Softening point (88% height), Half-sphere point (50% height) and Melting point (45% height). The values of these points are listed in Table 2, along with the trends in Figure 11-12. The finishing point of melting could be taken as the initial cylindrical sample becomes spherical under the action of the surface tension of the melt [8]. Adding MgO in the 5 wt% amount resulted in a decrease in the sintering, softening and half-sphere points. However, these values gradually increased afterwards (beyond x = 0.1). This trend was similar to that of the dilatometric results. The only difference between the two lies in the sample preparation; the dilatometric samples were obtained from the glazes which were already fired up to their maturation points whereas the melting behavior samples were simply consolidated pellets of starting mixtures. Different slopes indicated the different rate of melting and could be associated with the microstructural change within the glass structure itself [9]. The x = 0.15 sample was included in this melting behavior study in order to confirm the trend between x = 0.1 and 0.2. The unlisted values in Table 2 were from the unavailability of data due to the limit of firing temperatures (1300°C) conducted in this study. Analogous to this study, Wang *et al.* [5] examined the melting behavior of the glass-ceramic glaze by measuring the diameter of the pellet after firing. This method is an alternative to the height measurement as both height and flow diameter would be closely correlated. Their study reported the flow diameter to be largest at 5 wt% MgO, indicating the highest degree of melting. When increasing the amount of MgO, the flow diameter sharply dropped from 20.78 mm. to 18.36 mm; this physical change was indicative of increased melting points. These results were in the same trend as the dilatometric data listed in Table 1; given the role of network modifier at a small amount of MgO, both T_g and T_s initially decreased. However, both temperatures shifted their trends beyond 5 wt% MgO. Nevertheless, the current results implied that a large amount of MgO addition would hinder the melting capability, which was earlier visually observed by a dry, parched surface morphology of the obtained glazes.

To employ these results for creative works, testing the crawl glaze with coloring pigments was carried out. Considering how the glazes crawled in Figure 3, the x = 0.1 composition was selected as it yielded a surface with glossiness along with a clear occurrence of crawling. Figure 13 shows the tested samples with addition of common coloring oxides in the amount of 1 wt%. All five coloring oxides demonstrated colors typically found in any commonly used transparent glaze. However, there were some different features such as the size of the crawling region (island) and the porous structure. To validate a possible variation in color, commercial stains were also employed as shown in Figure 14. Unfortunately, all seven stains were not able to yield the colors corresponding to their original colors. This issue of alteration in color could likely be explained by the instability of these stains in the glaze with a very high content of MgO. It has been known among potters and ceramists that some pigments have their own environmental preferences. For example, malayaite-based pigments are not recommended to be used in a high-ZnO glaze [10]. Even for zircon-based compounds which are known to be one of the most stable, ZnO, $BaCO_3$ and dolomite were reported to degrade its color (yellow) [11]. It would not be surprising to obtain the similar color change in this study as MgO is also of an alkali-earth type with an oxidation state of 2+. Hence, obtaining color variation in this MgO-based crawl glaze is still a pending challenging issue for creating artistic works using a crawl glaze alone.

Table 1. Thermal expansion coefficient (α), T_g and T_s of the samples fired at 1200°C for 1 h.

$MgCO_3$ [wt%]	**Thermal expansion coefficient (α) within 200°C to 500°C [$1 \cdot °C^{-1}$]**	**T_g [°C]**	**T_s [°C]**
0	16.69×10^{-6}	745.2	835.7
2	15.31×10^{-6}	723.6	816.1
5	14.18×10^{-6}	710.1	805.1
7	13.73×10^{-6}	720.5	811.0
10	12.96×10^{-6}	725.1	823.5
20	11.76×10^{-6}	742.2	827.1

Table 2. The characteristic temperatures of the samples with different amounts of MgO addition fired between 1100°C and 1300°C for 1 h. The samples of M0, M5, M10, M15, M20, and M30 contained addition of MgO in the amounts of 0 wt%, 4 wt%, 10 wt%, 15 wt%, 20 wt%, and 30 wt%, respectively.

Characteristic points	**M0**	**M5**	**M10**	**M15**	**M20**	**M30**
Sintering point (95% height remaining)	920°C	853°C	874°C	926°C	981°C	1162°C
Softening point (88% height remaining)	1082°C	987°C	1048°C	1161°C	1211°C	1247°C
Half sphere point (50% height remaining)	1298°C	1235°C	1259°C	-	-	-
Melting point (45% height remaining)	-	1241°C	1269°C	-	-	-

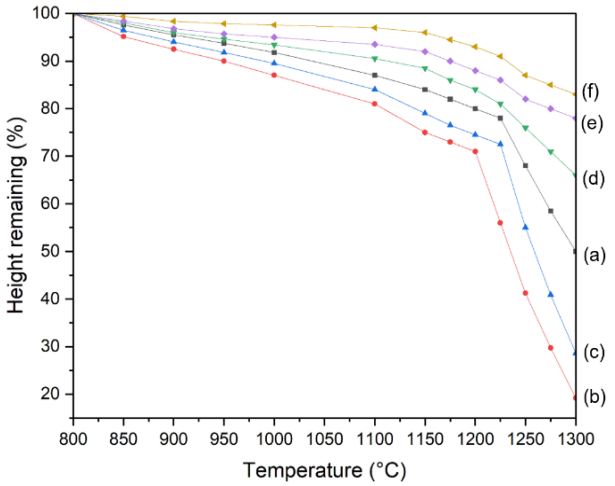

Figure 11. The melting profile of glaze samples with different amounts of MgO addition fired at 1200°C for 1 h. The height percentage was calculated relative to the initial height at 800°C. (a) 0 wt%, (b) 5 wt%, (c) 10 wt%, (d) 15 wt%, (e) 20 wt%, and (f) 30 wt%.

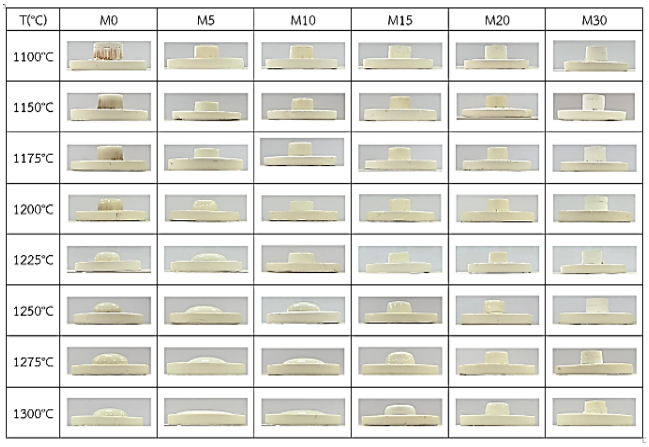

Figure 12. The glaze samples with different amounts of MgO addition fired between 1100°C and 1300°C for 1 h. Changes in shape indicated the level of maturation (melting). The samples of M0, M5, M10, M15, M20, and M30 contained addition of MgO in the amounts of 0 wt%, 5 wt%, 10 wt%, 15 wt%, 20 wt%, and 30 wt%, respectively.

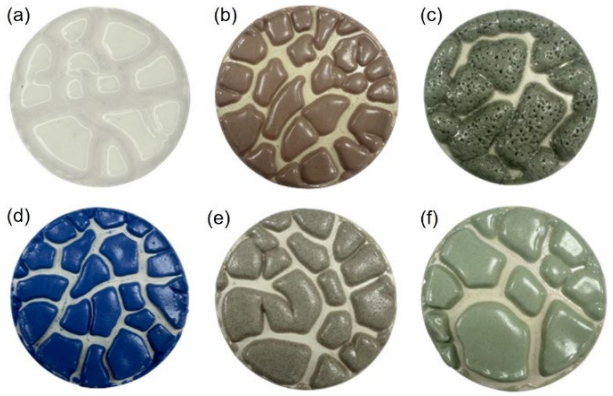

Figure 13. The glaze samples (10 wt% MgO) with addition of coloring oxides in the amount of 1 wt%. (a) Unadded, (b) Fe_2O_3, (c) CuO, (d) Co_3O_4 , (e) NiO, and (f) Cr_2O_3.

Figure 14. The glaze samples (10 wt% MgO) with addition of ceramic stains in the amount of 5 wt%. (a) Unadded, (b) Purple, (c) Blue, (d) Green, (e) Yellow, (f) Orange and (g) Red. All stains were from Amarin Ceramics.

4. Conclusions

Crawling in ceramic glazes, when excluding all physical imperfections of the glaze prior to firing, has been demonstrated in this study to be mainly caused by crystallization of several phases in the glass structure as evidenced by XRD and SEM. With MgO addition, alterations in the glass structure resulted in different behaviors among inherent

properties. A small amount of MgO (5 wt%) helped facilitate glaze melting through its role being a network modifier. Beyond this amount, MgO could not be dissolved in the glass structure under the current processing condition in this study, and it precipitated out as magnesium silicate due to interaction with SiO_2 in the sample. MgO addition beyond 5 wt% resulted a decrease in the coefficient of thermal expansion (down to 11.76×10^{-6} $1 \cdot ℃^{-1}$) for the x = 0.2 sample and increases in glass-transition temperature and softening temperature (742.2℃ and 827.1℃ for the x = 0.2 sample respectively; these were also accompanied by reduction in glaze maturation capability as evidenced by the melting behavior study. This dilatometric trend suggested a similarity with a glass-ceramic material within which reinforcing crystals enhanced the rigidity of the overall structure. Although MgO played a major role on inducing crawling, too much amount resulted in a parched, immature glaze which tended to peel off from the underlying clay substrate. The findings in this study could pave the way for a scientific guideline for investigation of crawling. To shed light on the mechanistic basis of the crawling phenomenon, external factors related to processing imperfections prior to glaze firing should be avoided. Only the intrinsic aspects pertinent to changes in the micro-structure should be considered. By understanding the fundamentals responsible for crawling, ceramists and artists would be able to precisely identify the appropriate additives, either to avoid or intentionally induce crawling, for their glaze systems.

Acknowledgements

This research is financially supported by Thailand Science Research and Innovation (TSRI) National Science, Research and Innovation Fund (NSRF) (Fiscal Year 2024)

References

[1] E. Youssef, N. Mostafa, J. E. Khoury, T. Merhej and R. Lteif, "Glaze surface defects causes and prevention controls," *Journal of Ceramic Science and Technology,* vol. 14, no. 1, pp. 1–10, 2023.

[2] D. Wattanasiriwech, and S. Wattanasiriwech, "Effect of particle size of glaze powder and thickness of glaze layer on glaze crawling for dolomite wares," *Chiang Mai Journal of Science,* vol. 33, no. 1, pp. 35–44, 2006.

[3] S. Junta, S. Mulinta, A. Saitan, and K. Ruammaitree, "Effect of Al_2O_3, $CaCO_3$ and $MgCO_3$ on physical properties of crawling Shino glaze in reduction atmosphere," *Key Engineering Materials,* vol. 608, pp. 258–363, 2014.

[4] J. Li, J. Liang, and L. Wang, "Effect of particle-size distribution on the surface appearance of glazed surface," *Journal of Thermal analysis Calorimetry,* vol. 115, pp. 1127–1131, 2014.

[5] S. Wang, Z. Bao, and L. Mian, "Effect of MgO on crystallization and properties of anorthite glass-ceramic glaze," *Journal of Ceramics,* vol. 44, no. 5, pp. 1024–1030, 2023.

[6] M. G. Rasteiro, T. Gassman, R. Santos, and E. Antunes, "Crystalline phase characterization of glass-ceramic glazes," *Ceramics International,* vol. 33, pp. 345–354, 2007.

[7] T. Mouri, and M. Enami, "Raman spectroscopic study of olivine-group minerals," *Journal of Mineralogical and Petrologgical Sciences,* vol. 103, pp. 100–104, 2008.

[8] R. L. Dumitrache, and I. Teoreanu, "Melting behavior of feldspar porcelain glazes," *Scientific Bulletin-University Politehnica of Bucharest,* vol. 68, no. 1, pp. 3–16, 2006.

[9] N. Yongvanich, T. Sirijan, P. Larptaweechai, and L. Chatchawong, "Reduction of maturation point in crystalline glaze through frit addition," *Monatshefte für Chemie/Chemical Monthly,* vol. 148, pp. 1329–1335, 2017.

[10] N. Yongvanich, C. Chanthanan, N. Ruennarong, and N. Suwanna, "Stability of malayaite pigments in high-ZnO ceramic glazes," *Key Engineering Materials,* vol. 772, pp. 90–94, 2018.

[11] N. Yongvanich, P. Soysom, and W. Ratkasemsak, "Synthesis of zircon pigments from rice husk ash and their performance in ceramic glaze," *Journal of Metals, Materials and Minerals,* vol. 33, no. 1, pp. 47–55, 2023.